A defect structure model of $LiNbO_3$:Sc_2O_3

1996 J. Phys.: Condens. Matter 8 6825

(http://iopscience.iop.org/0953-8984/8/37/005)

J. Phys.: Condens. Matter **8** (1996) 6825–6832. Printed in the UK

A defect structure model of $LiNbO_3$:Sc_2O_3

S Shimamura†, Y Watanabe†[+], T Sota†‡, K Suzuki†§, N Iyi‖, Y Yajima‖, K Kitamura‖, T Yamazaki¶, A Sugimoto¶ and K Yamagishi¶

† Department of Electrical, Electronics, and Computer Engineering, Waseda University, Shinjuku, Tokyo 169, Japan

‡ Advanced Research Centre for Science and Engineering, Waseda University, Shinjuku, Tokyo 169, Japan

§ Kagami Memorial Laboratory for Material Science and Technology, Waseda University, Shinjuku, Tokyo 169, Japan

‖ National Institute for Research in Inorganic Materials, Namiki 1-1, Tsukuba-shi, Ibaraki 305, Japan

¶ Corporate R & D Centre, Mitsui Mining & Smelting Co. Ltd, 1333-2 Haraichi, Ageo, Saitama 362, Japan

Received 9 April 1996, in final form 10 June 1996

Abstract. We have systematically studied the behaviour of the absorption bands due to the O–H bond-stretching vibration and its polarization characteristics in $LiNbO_3$:Sc_2O_3 with the use of well characterized crystals. It has been found that the O–H bond-stretching vibrational frequencies, ν(OH), have a strong correlation with Nb concentration in the crystals as in the case of MgO-doped $LiNbO_3$. The values of ν(OH) shift to the higher-frequency region when the Sc concentration in the crystal exceeds about 2.5 mol%. The magnitude of the frequency shift is smaller and the polarization dependence of the absorption bands due to ν(OH) is weaker in Sc_2O_3-doped $LiNbO_3$ than in MgO-doped $LiNbO_3$. These features are attributed to the difference of the charge between Sc^{3+} and Mg^{2+}. We have also proposed an ideal defect structure model for Sc_2O_3-doped $LiNbO_3$, which is based on the Li-site vacancy model as an intrinsic defect structure model. The observed behaviour of ν(OH) is consistently explained by the proposed defect structure model. This supports the justification of the extrinsic defect structure model based on the Li-site vacancy model for Sc_2O_3-doped $LiNbO_3$ as well as for MgO-doped $LiNbO_3$.

1. Introduction

Recently Yamamoto *et al* have reported that the optical damage of 1 mol% Sc_2O_3-doped $LiNbO_3$, which is denoted as $LiNbO_3$:Sc_2O_3 hereafter, is approximately two times smaller than that for non-doped $LiNbO_3$, referred to as just $LiNbO_3$ hereafter, as a function of laser irradiation time [1]. In this crystal, a 10 nm blue-shift of the fundamental absorption edge has been found but no discernible frequency shift of the absorption band due to the O–H bond-stretching vibration has been observed. They pointed out on the basis of those findings that Sc^{3+} and Mg^{2+} incorporation might proceed by a different mechanism. To the best of our knowledge, neither a systematic study on the absorption bands due to the O–H bond-stretching vibration nor a study on the defect structure in $LiNbO_3$:Sc_2O_3 has yet been performed.

[+] Present address: CPU & ASIC Design Section, Design Department, Ayase LSI Research Centre, LSI Division, NKK Corporation, 2596 Yoshioka, Ayase, Kanagawa 252, Japan.

0953-8984/96/376825+08$19.50

In our previous paper, hereafter referred to as I [2], we studied the intrinsic (extrinsic) defect structure of $LiNbO_3$ ($LiNbO_3$:MgO) combining the behaviour of ν(OH), i.e., the frequency of the O–H bond-stretching vibration, the polarization dependence of absorption bands due to ν(OH), Novak's empirical relation between ν(OH) and the hydrogen bond length, $R(O\cdots O)$ and/or r(O–H) [3], and the data on the chemical and structural analysis of the samples. We have found the following: (i) the hydrogen bonds are formed in the oxygen plane just above Nb^{5+} at the Nb site, hereafter abbreviated as Nb^{5+}_{Nb}; (ii) the values of ν(OH) have a strong correlation with the Nb concentration, [Nb], in the crystals; and (iii) the behaviour of ν(OH) reflects the defect structures and supports a Li-site vacancy model [4, 5] as the intrinsic defect structure model and the corresponding extrinsic one. The same extrinsic model has been proposed independently by Iyi *et al* [6]. We have also briefly predicted the behaviour of ν(OH) in $LiNbO_3$:Sc_2O_3 using the extrinsic defect structure model based on the Li-site vacancy model. To check the previous results and prediction and, consequently, to deal with the open problem mentioned before, it is desirable to study the behaviour of ν(OH) in $LiNbO_3$:Sc_2O_3.

In this paper, we have systematically studied the behaviour of ν(OH) in $LiNbO_3$:Sc_2O_3 to gain an insight into the defect structure of the crystals. As in the case of $LiNbO_3$:MgO, we have observed that there exists a threshold concentration of Sc over which the frequency shift of ν(OH) occurs, and the frequency shift of ν(OH) occurs only for $[Nb]/([Sc_2O_3] + [LiNbO_3]) < 1$, while both the value of the threshold concentration and the extent of the frequency shift observed in $LiNbO_3$:Sc_2O_3 are smaller than those in $LiNbO_3$:MgO. The polarization dependence of absorption bands due to ν(OH) on [Sc] has been found to be weak. The essential behaviour of ν(OH) obtained herein is consistent with the extrinsic defect structure model previously predicted [2]. The observed differences for $LiNbO_3$:MgO and $LiNbO_3$:Sc_2O_3 are attributed to the difference of the ionic charges for Mg^{2+} and Sc^{3+}. We will also discuss an ideal defect structure model for $LiNbO_3$:Sc_2O_3 based on a scenario of the Li-site vacancy model.

Table 1. Compositions of samples.

Sample	[Sc][a] (mol%)	Nb_2O_5:Li_2O:Sc_2O_3 (wt%)[b]
CG	0.00	90.4:9.57:0.00
Sc07	0.66	—
Sc13	1.32	—
Sc15	1.50	89.8:9.58:0.52
Sc27	2.66	—
Sc28	2.84	89.3:9.56:1.21
Sc32	3.19	89.3:9.47:1.30
Sc36	3.56	89.3:9.13:1.53

[a] $100 \times \{[Sc]/([LiNbO_3] + [Sc_2O_3])\}$. The values are those before melting.
[b] The values obtained from chemical analysis.

2. Experimental details

Eight single crystals doped with different Sc_2O_3 concentrations were prepared. All of the samples were grown by the Czochralski method. The Sc concentrations before melting are listed in table 1. For a reference, we used a non-doped sample with congruent composition. Among the samples, chemical analysis was performed for Sc15, Sc28, Sc32, and Sc36.

The chemical analysis was conducted as follows. The crushed samples were dissolved in HNO_3–HF solution in a closed Teflon vessel at 160 °C overnight. After filtering to separate the precipitated ScF_3, the resulting solution was passed through an anion exchanger for further separation of Li and Nb ions. The Li and Sc contents were analysed by inductively coupled plasma atomic spectrometry. Nb ions eliminated from the resin by the HCl–HF solution were precipitated by cupferron, and the precipitate was dried and incinerated. Weighing of the Nb_2O_5 yielded gave the Nb content. We performed the chemical analysis at least three times for each of the samples. The errors in the Li, Sc, and Nb contents are, respectively, less than ±0.01 wt%, ±0.05 wt%, and ±0.1 wt%.

The infrared, IR, transmittance and reflectance spectra were recorded using a Hitachi I-3000 grating spectrometer in the range from 3400 cm^{-1} to 3600 cm^{-1} at room temperature and in air. The spectral resolution was 2.0 ± 0.5 cm^{-1}. The absorption spectra were calculated taking account of multiple reflection. A wire grid polarizer was used for polarization measurements. In this case only the transmittance spectra were recorded to save time.

Table 2. Chemical formulae of the samples. □ denotes a vacancy.

Sample	Chemical formulae
CG	$Li_{0.951}\square_{0.039}Nb_{1.0098}O_{3.00}$
Sc15	$Li_{0.943}Sc_{0.0111}\square_{0.0419}Nb_{1.004}O_{3.00}$
Sc28	$Li_{0.930}Sc_{0.0254}\square_{0.0459}Nb_{0.999}O_{3.00}$
Sc32	$Li_{0.922}Sc_{0.0274}\square_{0.0516}Nb_{0.999}O_{3.00}$
Sc36	$Li_{0.908}Sc_{0.0331}\square_{0.0609}Nb_{0.998}O_{3.00}$

3. Results and discussion

Chemical compositions of the four samples for which chemical analysis was performed are listed in table 1 in units of weight per cent. The data on the chemical composition were used to calculate the chemical formulae. This was performed under the following assumptions: (i) no oxygen vacancy; (ii) charge neutrality; and (iii) no change of valence. The justification for these assumptions has been guaranteed from the analysis of $LiNbO_3$ and $LiNbO_3$:MgO [5, 6]. The chemical formulae so obtained are listed in table 2.

In figure 1 we show the absorption coefficients, α, measured using unpolarized light, for (a) [Sc] < 2.66 mol% and (b) [Sc] > 2.66 mol% , where the values of [Sc] are those before melting. For comparison, α for $LiNbO_3$ with congruent composition, CG, is also shown. It is seen from figure 1(b) that there exists a threshold concentration N_{th} over which ν(OH) shifts toward the higher-frequency region. This behaviour is similar to that in $LiNbO_3$:MgO. The spectra for samples Sc28 and Sc32 indicate that the values of [Sc] in those samples lie in the region just above N_{th}. The value of N_{th} in the crystal is estimated as about 2.5 mol% from the chemical analysis shown in table 2. Note that the scattering of data for Sc28 is merely due to the small sample size, and the integrated absorption intensity, i.e., the concentration of hydrogen bonds, n_{OH}, in the crystals, varies from sample to sample according to the growth conditions.

To estimate the values of ν(OH) causing the absorption bands and the corresponding n_{OH}, we have decomposed the absorption spectra into some spectra using the Lorentzian and/or the Gaussian lineshape functions, where ν(OH), the intensity and the half-width at half-maximum have been treated as fitting parameters. n_{OH} corresponding to each

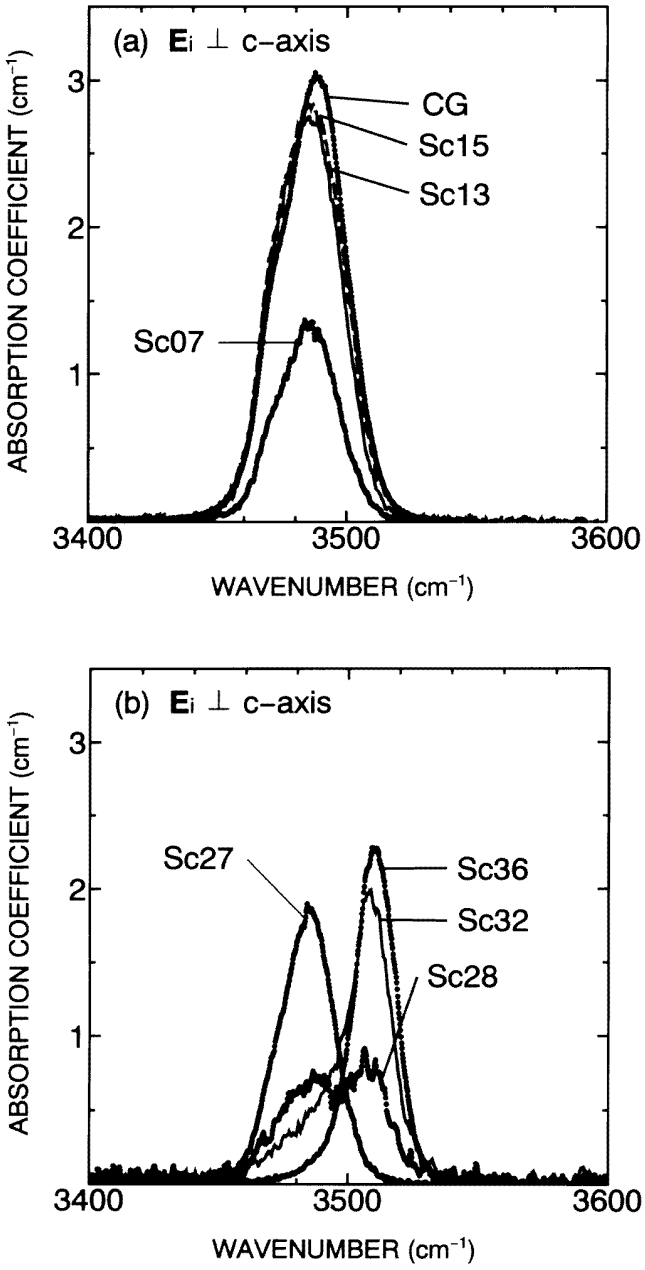

Figure 1. Dependencies of the absorption coefficients due to the O–H bond-stretching vibration on the frequency ν(OH) in (a) samples with [Sc] < 2.66 mol% and (b) those with [Sc] > 2.66 mol% , where the concentrations of Sc, [Sc], are for before melting. For comparison, the absorption coefficient is also shown for a non-doped sample with congruent composition.

decomposed spectrum has been calculated using the formula given by Klauer *et al* [7]. The values obtained for n_{OH} in each sample are found to be at most of the order of

10^{18} cm^{-3} and to be much smaller than the defect densities, as in the case for $LiNbO_3$ and $LiNbO_3$:MgO.

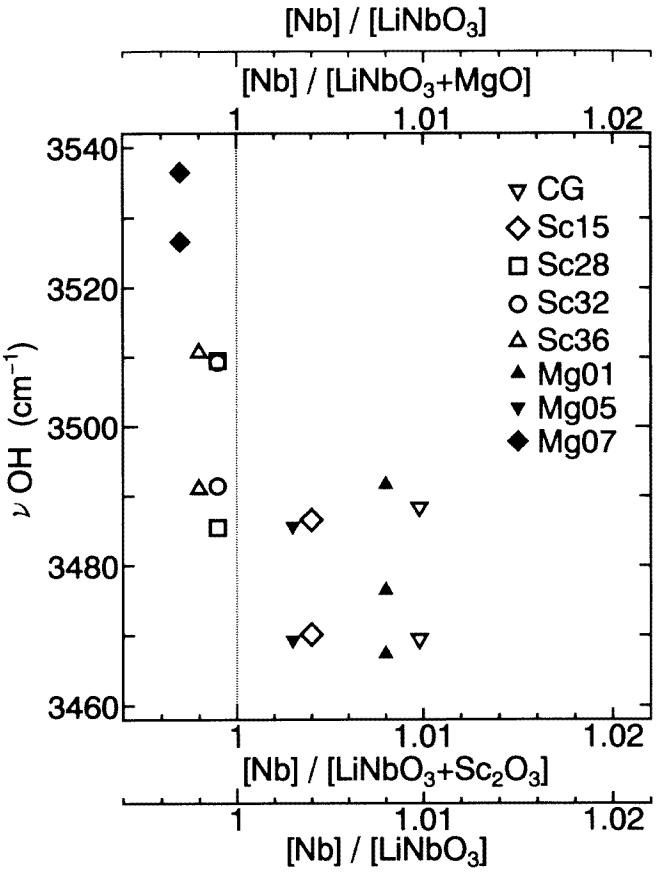

Figure 2. Dependencies of the O–H bond-stretching frequencies ν(OH) for each decomposed spectrum on [Nb] in $LiNbO_3$:Sc_2O_3 crystals. For comparison, dependencies of ν(OH) on [Nb] in $LiNbO_3$:MgO crystals are also shown; see references [2] and [6] for details. The chemical formulae for Mg01, Mg05 and Mg07 are $Li_{0.949}Mg_{0.0074}\square_{0.036}Nb_{1.008}O_{3.00}$, $Li_{0.896}Mg_{0.045}\square_{0.056}Nb_{1.003}O_{3.00}$, and $Li_{0.872}Mg_{0.071}\square_{0.060}Nb_{0.997}O_{3.00}$, respectively.

Figure 2 shows the dependence of ν(OH) on [Nb] in the crystals, where that for the samples CG, Mg01, Mg05, and Mg07 reported in I is also shown for comparison. The chemical formulae for Mg01, Mg05, and Mg07 are $Li_{0.949}Mg_{0.0074}\square_{0.036}Nb_{1.008}O_{3.00}$, $Li_{0.896}Mg_{0.045}\square_{0.056}Nb_{1.003}O_{3.00}$, and $Li_{0.872}Mg_{0.071}\square_{0.060}Nb_{0.997}O_{3.00}$ respectively [2, 6]. Figure 2 clearly indicates that the shift of ν(OH) toward the larger-frequency region occurs only in samples with $[Nb]/([LiNbO_3] + [Sc_2O_3]) < 1$ for $LiNbO_3$:Sc_2O_3. The correlation between ν(OH) and [Nb] in the crystals is the same as that found in $LiNbO_3$:MgO. It is also found that the values of shifted ν(OH) are about 3510 cm^{-1} for $LiNbO_3$:Sc_2O_3 and 3530 cm^{-1} for $LiNbO_3$:MgO. It follows from this that the change of r(O–H) seems to be smaller in $LiNbO_3$:Sc_2O_3 than in $LiNbO_3$:MgO.

The polarization dependencies of the integrated absorbance intensities calculated from the transmittance spectra for Sc07, Sc13, Sc27, and Sc36 are shown in figure 3. The inset

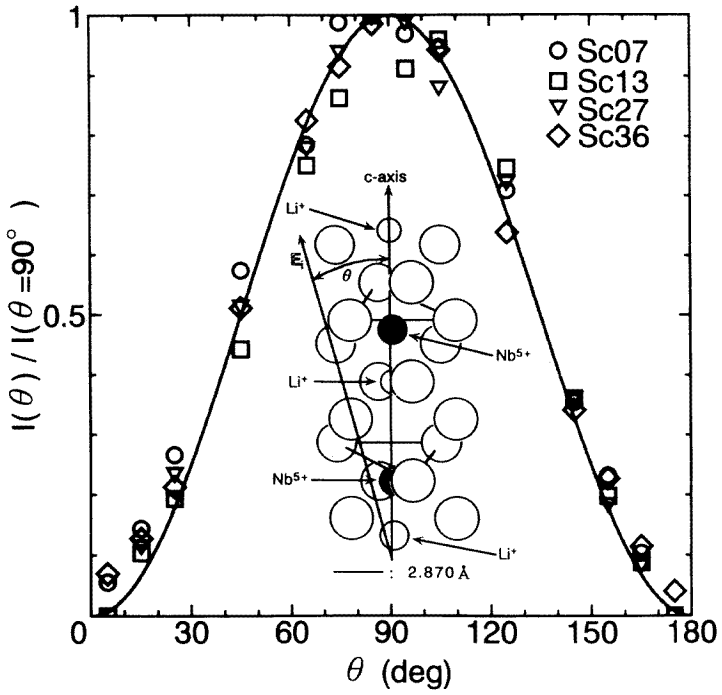

Figure 3. The polarization dependence of the integrated absorption intensities estimated from the transmittance spectra for $LiNbO_3$:Sc_2O_3. We define θ as the angle formed by the c-axis and the electronic field vector $\boldsymbol{E}_i$ of the light propagating perpendicular to the c-axis as illustrated in the inset.

in figure 3 shows a schematic illustration of the crystal structure and the definition of angle θ, where $\boldsymbol{E}_i$ indicates the electric field associated with the incident ray. The solid curve in figure 3 denotes the theoretically expected function, $\sin^2\theta$ [8]. It is found from figure 3 that the deviations from the expected function are small for all samples. Comparing figure 3 with figure 3(b) in I, we have found that the values for the angle between the direction of the O–H bonds and the plane perpendicular to the c-axis is smaller for $LiNbO_3$:Sc_2O_3 than for $LiNbO_3$:MgO.

Table 3. The defect structure model of $LiNbO_3$:Sc_2O_3.

[Sc]	Formula
0.0%	$[Li_{0.95}Nb_{0.01}\square_{0.04}][Nb]O_3$
	↓ Li/Nb = 0.94
2.0%	$[Li_{0.94}Sc_{0.02}\square_{0.04}][Nb]O_3$
	↓ Sc → Li site
100x%	$[Li_{1-3x}Sc_x\square_{2x}][Nb]O_3$
	↓ up to limit of Li/Nb ratio[a]

[a] Unfortunately the value is not known yet for $LiNbO_3$:Sc_2O_3. The value for $LiNbO_3$:MgO is 0.84.

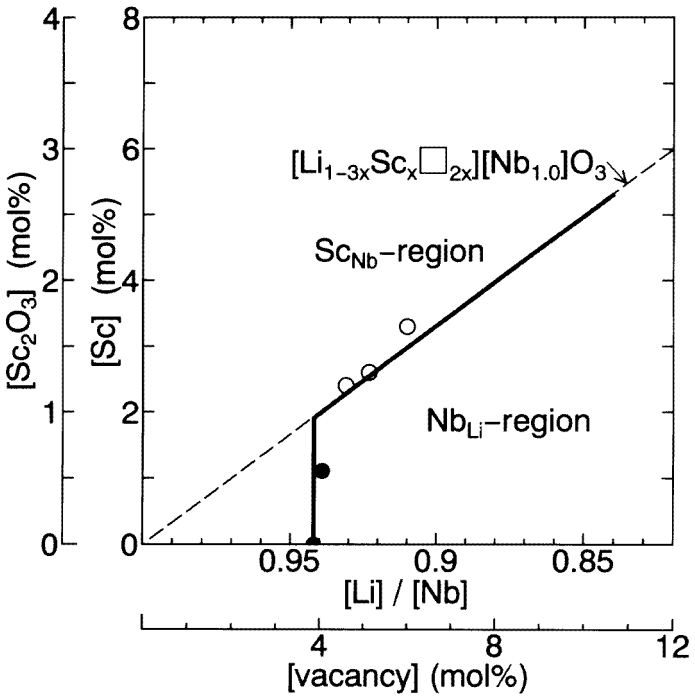

Figure 4. A schematic illustration of the defect structure model of $LiNbO_3$:Sc_2O_3. For comparison experimental data are also plotted, where solid circles and open circles indicate, respectively, samples with ν(OH) $\approx$ 3480 cm^{-1} and those with ν(OH) $\approx$ 3510 cm^{-1}.

The behaviour of ν(OH) in $LiNbO_3$:Sc_2O_3 observed herein matches that predicted in I. To get further insight, we consider an ideal defect structure model for $LiNbO_3$:Sc_2O_3 based on the experimental results and Li-site vacancy model as the intrinsic defect structure model. Before going on, we should recall the following. As shown in I, hydrogen enters in the oxygen triangle just above Nb_{Nb}^{5+} in the case of non-doped crystals and the situation does not change for crystals doped with impurities. The hydrogen bond is affected dominantly by the change of the Nb site from the fact that the distance between the oxygen and the nearest Nb_{Nb}^{5+} is shorter than that between the oxygen and the nearest Li_{Li}^{+}. For the case of congruent $LiNbO_3$ the excess Nb^{5+} is in the Li site and all vacancies needed for satisfying the charge neutrality are also in the Li site. The chemical formula is given by $[Li_{0.95}Nb_{0.01}\square_{0.04}][Nb_{1.0}]O_3$. When the concentration of Sc_2O_3 is below 2.5 mol% , no shift of ν(OH) is observed. This indicates that the environment surrounding the hydrogen bond does not significantly change and, thus, the Nb sites are hardly disturbed in comparison to the case for the congruent $LiNbO_3$. It follows that the Sc^{3+} introduced by doping enter not the Nb site but the Li site and simultaneously vacancies remain at the Li site. Assuming that the ratio [Li]/[Nb] is maintained as 0.94 in the first step, as in the case of $LiNbO_3$:MgO, complete replacement of Nb_{Li}^{5+} by Sc_{Li}^{3+} takes place at [Sc] = 2 mol% . The corresponding formula is written as $[Li_{0.94}Sc_{0.02}\square_{0.04}][Nb_{1.0}]O_3$. When further Sc^{3+} ions are introduced by doping, they replace the Li_{Li}^{+} up to some limiting value of the [Li]/[Nb] ratio which corresponds to the Nb-rich-side limit of the $LiNbO_3$ solid-solution range and should be determined experimentally. Unfortunately, to date, we do not know this value

for $LiNbO_3$:Sc_2O_3 because only a limited number of samples were available. Note that the value is 0.84 for $LiNbO_3$:MgO [6, 9]. Beyond this point, doped Sc^{3+} ions are expected to enter both the Nb and the Li site simultaneously, keeping the [Li]/[Nb] ratio constant. In table 3 an ideal scheme of Sc_2O_3 incorporation in congruent $LiNbO_3$ speculated on herein is given.

Figure 4 shows a diagram plotting the amount of [Sc] (and [Sc_2O_3]) against the [Li]/[Nb] ratio. The dashed diagonal line, which corresponds to a boundary line, denotes the formula $[Li_{1-3x}Sc_x\square_{2x}][Nb_{1.0}]O_3$ representing the state with neither Nb_{Li}^{5+} nor Sc_{Nb}^{3+}. Thus, the region above the line can be interpreted as the 'Sc_{Nb}^{3+} region' and that below as the 'Nb_{Li}^{5+} region'. The solid line shows the defect structure model given in table 2. As mentioned in the previous paragraph, we cannot draw the boundary line representing the Nb-rich-side limit of the $LiNbO_3$:Sc_2O_3 solid-solution range. Experimental data are also shown in figure 4 by solid and open circles. The former (latter) represents the samples with ν(OH) $\approx$ 3480 (3510) cm^{-1}. Figure 4 indicates that reasonable agreement is achieved between experiment and our defect structure model. So it seems that our structure model for $LiNbO_3$:Sc_2O_3 is appropriate. It is also reconfirmed that the behaviour of ν(OH) sensitively reflects the defect structure.

In figure 4 the information on the number of vacancies in the crystals is also shown. On increasing the Sc concentration, vacancies increase leading to the higher optical damage resistance [6, 10, 11]. Comparing figure 4 and figure 3 in [6], we find that a lower Sc concentration is sufficient for obtaining the same amount of vacancies in $LiNbO_3$:Sc_2O_3 as in $LiNbO_3$:MgO.

In summary, we have systematically studied the behaviour of ν(OH) in $LiNbO_3$:Sc_2O_3 using well characterized samples and confirmed that the previous predictions given by us are correct. We have also discussed the defect structure model, and found that the extrinsic defect structure model based on the Li-site vacancy model as the intrinsic defect structure model can consistently explain the experimental data.

References

[1] Yamamoto J K, Kitamura K, Iyi N, Kimura S, Furukawa Y and Sato M 1992 *Appl. Phys. Lett.* **61** 2156
[2] Watanabe Y, Sota T, Suzuki K, Iyi N, Kitamura K and Kimura S 1995 *J. Phys.: Condens. Matter* **7** 3627
[3] Novak A 1974 *Struct. Bonding* **18** 177
[4] Lerner P, Legras C and Dumas J P 1968 *J. Cryst. Growth* **3+4** 231
[5] Iyi N, Kitamura K, Izumi F, Yamamoto J K, Hayashi T, Asano H and Kimura S 1992 *J. Solid State Chem.* **101** 340
[6] Iyi N, Kitamura K, Yajima Y, Kimura S, Furukawa Y and Sato M 1995 *J. Solid State Chem.* **118** 148
[7] Klauer S, Wöhlecke M and Kapphan S 1992 *Phys. Rev.* B **45** 2786
[8] Kovács L, Polgár K and Capelletti R 1987 *Cryst. Lattice Defects Amorph. Mater.* **15** 115
[9] Grabmaier B C and Otto F 1986 *J. Cryst. Growth* **79** 682
[10] Anghert N B, Pashkov V A and Solov'yeva N M 1972 *Zh. Eksp. Teor. Fiz.* **26** 1666
[11] Furukawa Y, Sato M, Kitamura K, Yajima Y and Minakata M 1992 *J. Appl. Phys.* **72** 3250